Available online at www.sciencedirect.com
SCIENCE DIRECT
Physica D 218 (2006) 56–69
PHYSICA D
www.elsevier.com/locate/physd

Phase compactons

Arkady Pikovsky[a,*], Philip Rosenau[b]

[a] *Department of Physics, Potsdam University, 14415 Potsdam, Germany*
[b] *School of Mathematics, Tel Aviv University, 69978 Tel Aviv, Israel*

Received 30 December 2005; received in revised form 7 April 2006; accepted 11 April 2006
Available online 22 May 2006
Communicated by A. Doelman

Abstract

We study the phase dynamics of a chain of autonomous, self-sustained, dispersively coupled oscillators. In the quasicontinuum limit the basic discrete model reduces to a Korteveg–de Vries-like equation, but with a *nonlinear dispersion*. The system supports compactons – solitary waves with a compact support – and kovatons – compact formations of glued together kink–antikink pairs that propagate with a unique speed, but may assume an arbitrary width. We demonstrate that lattice solitary waves, though not exactly compact, have tails which decay at a superexponential rate. They are robust and collide nearly elastically and together with wave sources are the building blocks of the dynamics that emerges from typical initial conditions. In finite lattices, after a long time, the dynamics becomes chaotic. Numerical studies of the complex Ginzburg–Landau lattice show that the non-dispersive coupling causes a damping and deceleration, or growth and acceleration, of compactons. A simple perturbation method is applied to study these effects.

Keywords: Lattice of nonlinear oscillators; Phase dynamics; Compacton

1. Introduction

The subject matter of this paper unifies two principal fields of nonlinear science: coupled self-sustained oscillators and soliton theory. Coupled autonomous oscillators have been a subject of interest since the discovery of their synchronization by Huygens [1]. A theoretical understanding of this phenomenon is almost one hundred years old [2]; since then different features of coupled oscillators have attracted considerable attention (see, e.g., [3,4]). When the coupling of periodic self-sustained oscillators is weak it can be described in the phase approximation [5], where only a variation of oscillator phases enters into play. For two coupled oscillators this leads to an Adler-type equation [6]. The corresponding phase models are widely used for a description of oscillator lattices [7–11] and globally coupled ensembles [5,12–15].

The phase approximation for coupled oscillators requires the coupling strength to be small compared to the smallest, in the absolute sense, negative Lyapunov exponent. One may then consider the 'amplitude' perturbations as slaved entities. In the absence of coupling the resulting phase equations have only zero Lyapunov exponents, therefore *the dissipative or conservative nature of the phase dynamics will solely depend on the particulars of the coupling*. In studies which focus on synchronization properties of oscillators, it is natural to assume that the coupling is dissipative which thus tends to equalize the phases. Adequately strong coupling then leads to a synchronous state with a uniform phase of a lattice or a network, if the coupling is attractive, or to an anti-phase lattice, if the coupling is repulsive. Notably, certain types of coupling lead to a conservative dynamics. A prominent example being that of a splay state in a globally coupled ensemble of oscillators [16–20].

In contradistinction to previous studies, in the present work we consider the dynamics of a one-dimensional lattice, a chain, of oscillators with a dispersive coupling. A multicore fiber laser [21], where individual self-oscillating lasers are arranged in a ring, may be a realization of such a lattice. Another physical example, an array of Josephson junctions, will be discussed below. Since both the local phase dynamics and the coupling are non-dissipative, such a system shares many

* Corresponding author. Tel.: +49 331 977 1472.
E-mail address: pikovsky@stat.physik.uni-potsdam.de (A. Pikovsky).

0167-2789/$ - see front matter
doi:10.1016/j.physd.2006.04.015

properties with Hamiltonian lattices, in particular the phase volume is conserved. This means that if stable synchronized states are admissible, they are not attractors, and the dynamics is expected to be similar to that of the well-known Hamiltonian examples, like the sine-Gordon lattice, for which the basic building blocks are traveling solitary waves like pulses or kinks, that on integrable lattices collide elastically (see, e.g., [22,23]), while in non-integrable cases eventually give way to chaos.

In recent years two new concepts have significantly enlarged our understanding of nonlinear processes in Hamiltonian lattices and fields. One concept introduces localized periodic breathers in lattices [24]. The other introduces excitations in genuinely nonlinear lattices and wave equations. Unlike the usual solitons that have exponential, or algebraic, tails, the corresponding traveling waves have compact or almost compact support. These waves, the **compactons**, have been introduced by one of us [25,26] and put forward in [27–35]. Typically, compacton-bearing PDE equations (or spatially discrete equations on a lattice) are non-integrable, at least in the conventional sense, yet their remarkable robustness seems to have very little to do with the conventional solitonic integrability and appears to originate in the nonlinear mechanism which induces their compactness. Many of the underlying equations of motion do not have an energy integral and some may, under certain conditions, generate exploding solutions. Nevertheless, typical numerical simulations show that an initial perturbation of a finite span decomposes into a set of compactons. As an example we mention a recent modeling of DNA opening with one-dimensional Hamiltonian lattices [36]. Other examples include a compression wave in a granular chain [37–41] and sedimentation of particles in dilute suspensions [42].

In the present paper we study compactons in a chain of dispersively coupled nonlinear self-sustained oscillators (a short report was presented in [43]). In Section 2 we derive the basic model of dispersively coupled phase equations. In particular, we show that such a model emerges naturally in a chain of Ginzburg–Landau oscillators. Some general features of our model are presented in Section 3 where we derive in the quasicontinuum approximation a genuinely nonlinear PDE to describe the dynamics on a lattice which for small amplitudes reduces to the K(2, 2)-model for compactons [26]. In Section 4 we present the solitary solutions of the derived PDE and show that there are two types of compact waves: the usual compactons (solitary waves with a compact support) and kovatons (flat-top compactons or glued compact kinks). The corresponding solitary traveling solutions on the lattice are found numerically using an iterative algorithm due to Petviashvili. We show that *the exactly compact front is replaced with a superexponential tail where the discrete effects are essential*. This effect is confined to a very thin boundary layer which shrinks to a singular point in the quasicontinuum limit. In Section 5 we present numerical simulations of the dynamics on the lattice: evolution of an initial pulse, collisions of compactons and kovatons and other types of waves. In Section 6 we consider finite lattices and demonstrate the emergence of a spatio-temporal chaos of Hamiltonian type. In Section 7 we step beyond the phase approximation and show that compactons and kovatons can be also observed in the Ginzburg–Landau lattice. Here, however, additional small dissipative terms arise and lead to the decay, or growth, of compactons; these effects are addressed using a perturbation method.

2. The basic model

2.1. Phase lattice and variety of couplings

An autonomous periodic self-sustained oscillator with frequency ω can be characterized by the phase φ that obeys $\frac{\mathrm{d}\varphi}{\mathrm{d}t} = \omega$. An equation for weakly coupled oscillators may be derived in two steps (see [4,5] for details). First, one uses a smallness of the coupling compared to the smallest, in the absolute sense, negative Lyapunov exponent of the oscillator. This allows us to write equations for the phase evolution on a perturbed limit cycle. For the lattice of identical oscillators these equations read

$$\frac{\mathrm{d}\varphi_n}{\mathrm{d}t} = \omega + \tilde{q}(\varphi_{n-1}, \varphi_n) + \tilde{q}(\varphi_{n+1}, \varphi_n). \tag{1}$$

Here $\tilde{q}$ is a coupling function 2π-periodic in each argument. In the second step the smallness of the coupling compared to the frequency ω is used to average the r.h.s. of (1). Then only the 'slow' part of $\tilde{q}$ remains and is a function of phase differences:

$$\frac{\mathrm{d}\varphi_n}{\mathrm{d}t} = \omega + q(\varphi_{n-1} - \varphi_n) + q(\varphi_{n+1} - \varphi_n), \tag{2}$$

where $q(\varphi + 2\pi) = q(\varphi)$. Introducing new variables

$$v_n = \varphi_{n+1} - \varphi_n, \tag{3}$$

we rewrite the phase equations as

$$\frac{\mathrm{d}v_n}{\mathrm{d}t} = q(-v_n) + q(v_{n+1}) - q(-v_{n-1}) - q(v_n). \tag{4}$$

Since the frequency does not appear in (4), rescaling the time we may consider the coupling function q to be of order one.

Since in general any function q can be represented as a sum of its odd and even parts, we write q as $q(v) = q^o(v) + q^e(v)$ to obtain

$$\begin{aligned}\frac{\mathrm{d}v_n}{\mathrm{d}t} &= q^e(v_{n+1}) - q^e(v_{n-1}) + q^o(v_{n+1}) \\ &\quad + q^o(v_{n-1}) - 2q^o(v_n) \\ &= \nabla_d q^e(v) + \Delta_d q^o(v),\end{aligned} \tag{5}$$

where Δ_d and ∇_d are the discrete Laplacian and nabla operators, respectively:

$$\Delta_d f = f_{n+1} + f_{n-1} - 2f_n, \quad \nabla_d f = f_{n+1} - f_{n-1}. \tag{6}$$

Typical and probably the simplest choice for the coupling is $q(\varphi) = \sin\varphi$. This odd coupling is dissipative and leads to the system $\dot{v}_n = \Delta_d \sin(v)$ that has the synchronous state $v_n = 0$ as an attractor. We, on the other hand, shall restrict our attention to a purely even coupling function, yielding

$$\frac{\mathrm{d}v_n}{\mathrm{d}t} = q(v_{n+1}) - q(v_{n-1}) = \nabla_d q(v) \tag{7}$$

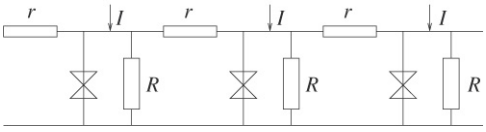

Fig. 1. An array of resistively coupled Josephson junctions.

(hereafter we shall for brevity omit the index e). This coupling may be considered as the dispersive one, because Eq. (7) conserves the phase volume and thus has no attractors and in the quasicontinuum limit (see Section 3 below) it induces a dispersive effect. Hereafter we shall almost exclusively limit our analysis to the particular case $q(v) = \cos v$ (which also seems to be the simplest one as it naturally emerges in applications, but it is not generic because it has certain additional symmetries) and thus:

$$\frac{\mathrm{d}v_n}{\mathrm{d}t} = \cos v_{n+1} - \cos v_{n-1} = \nabla_d \cos v. \tag{8}$$

2.2. An example: Complex Ginzburg–Landau lattice

As an example we consider a complex Ginzburg–Landau lattice (it will be considered in a greater detail in Section 7)

$$\frac{\mathrm{d}A_k}{\mathrm{d}t} = A_k(1 - (1 + ic_1)|A_k|^2) + (c_2 + ic_3) \times (A_{k-1} + A_{k+1} - 2A_k). \tag{9}$$

Note that Eq. (9), for complex amplitudes of oscillations A, are already written in the rotating (with the oscillation frequency) frame of reference and need not be averaged, but still have to be reduced into a single equation for the phase. To this end we assume the coupling coefficients c_2 and c_3 to be small compared with the Lyapunov exponent on the limit cycle, which in our case is -2. Then to a leading order in c_2, c_3, $|A_n| = 1$. The reduction to the phase equation, carried out in the Appendix, yields in this order

$$\dot{v}_k = (c_3 - c_1c_2)\nabla_d \cos v_k + (c_2 + c_1c_3)\Delta_d \sin v_k. \tag{10}$$

Thus the dispersive coupling is proportional to $c_3 - c_1c_2$ while the odd term representing the dissipative coupling is proportional to $c_2 + c_1c_3$. As we shall see in Section 7, in the next order in c_2 and c_3 more complex dissipative corrections of (10) emerge.

2.3. An array of Josephson junctions

As an example of a concrete physical setup we consider a one-dimensional array of resistively coupled Josephson junctions (see Fig. 1), fed by a dc current I.

Each junction is characterized by the Josephson phase ψ_n, and the balance of currents gives the governing equations

$$I = \frac{\hbar}{2eR}\dot{\psi}_n + I_c \sin\psi_n + \frac{1}{r}(V_n - V_{n-1} + V_n - V_{n+1}) = \frac{\hbar}{2eR}\dot{\psi}_n + I_c \sin\psi_n + \frac{\hbar}{2er}(2\dot{\psi}_n - \dot{\psi}_{n+1} - \dot{\psi}_{n-1}),$$

where the voltages are $V_n = \frac{\hbar}{2e}\dot{\psi}_n$ and the Josephson currents are $I_c \sin\psi_n$ (the same system describes an array of coupled overdamped pendula).

Following Ref. [44] we introduce a uniformly rotating phase ϕ via $\tan\frac{\phi}{2} = \sqrt{\frac{I-I_c}{I+I_c}}\tan(\frac{\psi}{2} + \frac{\pi}{4})$ and using the identity $(I - I_c\sin\psi)(I - I_c\cos\phi) = I^2 - I_c^2$ obtain

$$\dot{\phi}_n = \omega_0 + \frac{R}{r}\left(\dot{\phi}_{n+1}\frac{I - I_c\cos\phi_n}{I - I_c\cos\phi_{n+1}} + \dot{\phi}_{n-1}\frac{I - I_c\cos\phi_n}{I - I_c\cos\phi_{n-1}} - 2\dot{\phi}_{n+1}\right),$$

where $\omega_0 = \frac{2eR}{\hbar}\sqrt{I^2 - I_c^2}$ is the frequency of non-coupled junctions, assumed to be large. Now we assume that the coupling parameter R/r is small, write $\phi = \omega_0 t + \theta$, and to the first order in the coupling strength obtain

$$\dot{\theta}_n = \omega_0\frac{R}{r}\left(\frac{I - I_c\cos(\omega_0 t + \theta_n)}{I - I_c\cos(\omega_0 t + \theta_{n+1})} + \frac{I - I_c\cos(\omega_0 t + \theta_n)}{I - I_c\cos(\omega_0 t + \theta_{n-1})} - 2\right).$$

The averaging over the period of fast oscillations $2\pi/\omega_0$ finally yields the equation (2) with the cos coupling function

$$\frac{\mathrm{d}\theta_n}{\mathrm{d}t} = \omega_0\frac{R}{r}\left(\frac{I - \sqrt{I^2 - I_c^2}}{\sqrt{I^2 - I_c^2}}\right) \times [\cos(\theta_{n+1} - \theta_n) + \cos(\theta_{n-1} - \theta_n) - 2].$$

3. General properties of the basic model

We now discuss the basic properties of our model (7). An infinite lattice is assumed. The effect of boundaries will be discussed in Section 6.

3.1. Conservation laws and symmetries

We note first that since the divergence $\frac{\partial\dot{v}_n}{\partial v_n}$ vanishes, our system is Liouvillean. Next, one easily verifies the following conservation laws:

$$I_1 = \sum_n v_n, \tag{11}$$

$$I_2 = \sum_n (-1)^n v_n, \tag{12}$$

$$I_3 = \sum_n Q(v_n), \quad \text{where } Q(v) = \int_0^v q(u)\mathrm{d}u. \tag{13}$$

These conservation laws are valid on an infinite lattice. Finite lattices are discussed in Section 6 where based on numerics we argue that no additional conservation laws are available.

In addition to the a priori assumed parity $q(v) = q(-v)$, system (7) is reversible (for a discussion of reversibility in chains of oscillators see [11]). This means that there exists an involution $\mathcal{R} : \mathcal{V} \to \mathcal{V}$ which, together with the time reversal map $\mathcal{T} : t \to -t$, leaves the system invariant. (Involution means that $\mathcal{R}^2 = \mathcal{I} =$ is an identity, and $\mathcal{V}$ is the set of

variables.) In the case of system (7) two possible involutions lead to reversibility

$$\mathcal{R}_1 : v_n \to v_{-n} \quad \text{and} \quad \mathcal{R}_2 : v_n \to -v_n. \tag{14}$$

Moreover, system (7) remains invariant under the involution

$$\mathcal{R}_3 = \mathcal{R}_1\mathcal{R}_2 : v_n \to -v_{-n}. \tag{15}$$

Additional symmetries of the coupling function $q(v)$ may result in corresponding symmetries of (7). In particular, since $q(v) = \cos v$ implies $q(\pi + v) = -q(v)$, in this case (7) is invariant under the involution

$$\mathcal{R}_4 : v_n \to \pi + v_{-n}. \tag{16}$$

3.2. A small-amplitude regime

Any constant $v_n = V$ is a solution of (7). For a small perturbation $\tilde{v}_n = v_n - V$ we have

$$\frac{\mathrm{d}\tilde{v}_n}{\mathrm{d}t} = q'(V)(\tilde{v}_{n+1} - \tilde{v}_{n-1}). \tag{17}$$

If $q'(V)$ vanishes, there is no evolution in the linear approximation and one has to consider nonlinear contributions. In particular, for an even 2π-periodic function $q'(0) = q'(\pi) = 0$, thus the perturbations of the homogeneous states $V = 0$ and $V = \pi$ essentially evolve nonlinearly. In the simplest case wherein the extrema of $q(u)$ are quadratic, say $q(u) = \cos u$, instead of (17) we obtain

$$\frac{\mathrm{d}\tilde{v}_n}{\mathrm{d}t} = -\frac{1}{2}(\tilde{v}_{n+1}^2 - \tilde{v}_{n-1}^2). \tag{18}$$

Eq. (18) is invariant under a scaling transformation

$$\tilde{v} \to a\tilde{v}, \qquad t \to \frac{t}{a}, \tag{19}$$

which implies that low amplitude structures evolve very slowly. This effect will come into play in Section 5.

Remarkably, Eq. (18) admits a special analytic solution of the form $\tilde{v}_n = A(t)\sin\frac{2\pi n}{3}$. Indeed, using this form in (18) yields

$$\begin{aligned}\frac{\mathrm{d}A}{\mathrm{d}t}\sin\frac{2\pi n}{3} &= \frac{A^2}{2}\left(\sin^2\frac{2\pi(n-1)}{3} - \sin^2\frac{2\pi(n+1)}{3}\right)\\ &= \sqrt{3/16}A^2\sin\frac{2\pi n}{3}.\end{aligned}$$

Thus this particular mode does not induce harmonics or subharmonics and its amplitude evolves according to

$$\frac{\mathrm{d}A}{\mathrm{d}t} = \sqrt{3/16}A^2,$$

yielding an explosive solution

$$A(t) = \frac{A_0}{1 - \sqrt{3/16}A_0\cdot(t - t_0)}.$$

Thus a very small component can grow until the nonlinearity of the full equation (7) slows it down. Note that this solution has no continuous counterpart. The existence of such an 'explosive mode' means that the trivial state $v_n = 0$ in Eq. (7) is rather sensitive to small perturbations. As we shall see, numerics confirms such explosions.

3.3. The quasicontinuous approximation (QCA)

In a quasicontinuous approximation, denoting the spatial step by h, we approximate the discrete operators (6) with spatial derivatives:

$$\nabla_d = 2h\left[\frac{\partial}{\partial x} + \frac{h^2}{6}\frac{\partial^3}{\partial x^3}\right], \quad \Delta_d = h^2\frac{\partial^2}{\partial x^2}.$$

The resulting equation is

$$\frac{\partial v}{\partial t} = 2h\left[\frac{\partial}{\partial x} + \frac{h^2}{6}\frac{\partial^3}{\partial x^3}\right]q(v). \tag{20}$$

We stress that Eq. (20) is not an asymptotic version of the lattice problem. Once the spatial length is normalized using the lattice length, the small parameter is eliminated and higher order terms are small to the extent that higher order gradients are small. Clearly, at the edge of a compact entity this cannot be true because the solution ceases to be analytical. Thus, depending on the degree of smoothness at the edge (which depends on the prevailing nonlinearity), starting with a certain derivative, all higher gradients will not be small and may even diverge. Thus no matter how good the continuum approximation may be elsewhere, at the edge it cannot describe the lattice well. Yet the issue is 'miraculously' resolved for, as we shall shortly see, though on the lattice the compact edge is replaced by a formally infinite tail, *this tail decays at a super exponential rate* and thus after about three discrete nodes it is completely negligible. Thus, the singularity of the continuum is a trace of an extremely localized discrete boundary layer which, as one approaches continuum, collapses into a singular manifold. This phenomenon can be compared to the viscous kinetic boundary layer in a gas which in the continuum, non-viscous, limit is replaced by a shock jump. The respective solutions are mathematically referred to as *weak solutions*. Since in our case the solution is continuous and only the gradients undergo a jump, our solutions could be viewed as *weakly weak solutions*. In light of what we have just stated, it is indeed remarkable that Eq. (20), embedded with only first correction in the discrete parameter, approximates the original problem so well.

4. Traveling waves

4.1. Traveling waves in QCA: Compactons and kovatons

We now set $h = 1$ and consider the traveling wave solutions of the quasicontinuum approximation (20):

$$\frac{\partial v}{\partial t} = \left(2\frac{\partial}{\partial x} + \frac{1}{3}\frac{\partial^3}{\partial x^3}\right)q(v). \tag{21}$$

We look for traveling waves $v = v(s) = v(x - \lambda t)$ on the trivial background $V = 0$.

Using the traveling wave ansatz in (21) and integrating once, we obtain

$$\lambda v + 2(q(v) - q(0)) + \frac{1}{3}\frac{\mathrm{d}^2}{\mathrm{d}s^2}q(v) = 0. \tag{22}$$

The integration constant $q(0)$ assures that the 'effective force' $\lambda v + 2(q(v) - q(0))$ vanishes at $v = 0$. Note that if in addition to $v = 0$ the derivative $q'(v)$ also vanishes at, say, $v = v_*$, then v_* is also a critical point of the system, and the 'effective force' has to vanish at this point as well. This may, as at $v = 0$, happen without any additional constrain on the 'effective force', or may have to be enforced via the choice of the only remaining free parameter — the speed λ. In the second case the condition on the 'effective force' invokes

$$\lambda = \lambda_* \equiv 2\frac{q(0) - q(v_*)}{v_*}. \tag{23}$$

We now multiply (22) with $\frac{\mathrm{d}q}{\mathrm{d}s}$ and integrate again, to obtain

$$\lambda\,[vq(v) - Q(v)) + (q(v) - q(0)]^2 + \frac{1}{6}\left(\frac{\mathrm{d}q}{\mathrm{d}s}\right)^2 = 0 \tag{24}$$

where Q is defined in (13) and the integration constant is chosen to ensure that the 'potential part' vanishes at $v = 0$. We now rewrite Eq. (24) as

$$(q')^2\left[\frac{1}{2}\left(\frac{\mathrm{d}v}{\mathrm{d}s}\right)^2 + U(v)\right] = 0, \tag{25}$$

with the 'potential' $U(v)$ being defined as

$$U(v) = 3\frac{(q(0) - q(v))^2 + \lambda[vq(v) - Q(v)]}{(q'(v))^2}. \tag{26}$$

Note that in spite of the apparent singularity at $v = 0$, the potential U may in fact be non-singular there.[1] Suppose that for small v, $q(v) \approx q(0) + av^\alpha$. Thus

$$U(v) \approx 3\left(\alpha^{-2}v^2 + \frac{\lambda}{\alpha(\alpha+1)a}v^{3-\alpha}\right). \tag{27}$$

Thus for $\alpha \le 3$ the potential is bounded at $v = 0$. If the additional singularity v_* at which $q'(v_*) = 0$ enters, a finiteness of the potential leads to the condition on the speed λ:

$$\lambda_{**} = \frac{(q(0) - q(v_*))^2}{Q(v_*) - v_*q(v_*)}. \tag{28}$$

Note that since in general $\lambda_{**} \neq \lambda_*$, thus a solution with a nonsingular potential both at $v = 0$ and $v = v_*$ is impossible. However, if the relation

$$Q(v_*) \equiv \int_0^{v_*} q(u)\mathrm{d}u = \frac{q(0) + q(v_*)}{2}v_* \tag{29}$$

holds (see (23)), then $\lambda_{**} = \lambda_*$. In particular, for $q(v) = \cos v$ (29) holds and both critical speeds coincide! Note that the presence of the integral makes condition (29) nonlocal.

[1] The fact that the potential is infinite does not preclude the existence of compactons. It implies, however, that the gradients at the edge will be infinite (as is the case for K(4, 4) [26]).

For a typical even function $q(v)$, one has $\alpha = 2$ in (26). Then for small amplitude solutions one can rewrite (25) as

$$v^2\left[\frac{1}{2}\left(\frac{\mathrm{d}v}{\mathrm{d}s}\right)^2 + \frac{\lambda}{2a}v + \frac{3}{4}v^2\right] = 0. \tag{30}$$

The bracket expresses 'conservation of energy' for a motion in a quadratic potential and admits harmonic solutions. A symmetric solution with a minimum at $v = 0$ is

$$v(s) = -\frac{\lambda}{3a}\left(1 + \cos\sqrt{\frac{3}{2}}s\right) = -\frac{2\lambda}{3a}\cos^2\left(\sqrt{\frac{3}{8}}s\right). \tag{31}$$

The trough of this solution touches zero, where the trivial state $v = 0$ is also a solution. Usually, one cannot match two different solutions of an ODE. However, in our problem $v = 0$ is a singular point where the highest order operator degenerates and the solution's uniqueness is lost. We thus combine these two solutions and obtain a composite solution — the compacton

$$v(s) = \begin{cases} -\dfrac{\lambda}{3a}\left(1 + \cos\sqrt{\dfrac{3}{2}}s\right) & \text{if } |s| \le \pi\sqrt{\dfrac{2}{3}}, \\ 0 & \text{if } |s| > \pi\sqrt{\dfrac{2}{3}}. \end{cases} \tag{32}$$

Note that the compacton's amplitude is proportional to its velocity λ. This is in full agreement with the scaling of solutions for small amplitudes, see (19).

In a similar way we construct a compacton for the full equation (25). In the particular case of $q(v) = \cos v$, $Q(v) = \sin v$ and Eq. (25) takes the form

$$\sin^2 v\left[\frac{1}{2}\left(\frac{\mathrm{d}v}{\mathrm{d}s}\right)^2 + U(v)\right] = 0, \tag{33}$$

with the potential being

$$U(v) = 3\frac{(\cos v - 1)^2 + \lambda(v\cos v - \sin v)}{\sin^2 v}. \tag{34}$$

Eq. (33) has a singularity both at $v = 0$ and $v = \pi$. In general, insofar as $v < \pi$, the maximal amplitude v_m of the compacton is found demanding that $U(v_m) = 0$. This renders the amplitude–velocity relation

$$\lambda = \frac{(\cos v_m - 1)^2}{\sin v_m - v_m\cos v_m}. \tag{35}$$

If we intend to integrate up to $v = \pi$, the second singularity of the system, we have to request that $U(v = \pi) = 0$ as well, which in turn imposes a critical wave speed λ:

$$\lambda_c = \lambda_{**} = \frac{(\cos\pi - 1)^2}{\sin\pi - \pi\cos\pi} = \frac{4}{\pi}. \tag{36}$$

This wave speed coincides with critical velocities defined in (23) and (28). Since at λ_c the potential is symmetric $U_c(v) = U_c(\pi - v)$, the corresponding kink which connects the singularities $v = 0$ and $v = \pi$ is also symmetric. This solution, as in (32), may be matched with the uniform states

$v = 0$ and $v = \pi$ and yields a *compact traveling kink*. Note also that due to symmetry $v \to \pi - v$, the kink connecting the singularity at $v = \pi$ with the one at $v = 0$ has the same velocity. Thus it is possible to construct a solution consisting of two kinks separated by an arbitrary finite width. Since the resulting compact kink–antikink pair looks like a compacton with a flat top, it has been named by us *kovaton* (from the Hebrew 'kova' for a hat) in Ref. [43], and we shall continue to refer to these flat-top compactons as kovatons. The explicit form of a compacton and of a kovaton can be found numerically either by solving Eq. (25) or solving directly the second-order equation (22). This will be carried out in the next subsection.

4.2. Traveling waves on a lattice

We remind the reader that the discrete problem is the original entity, with the continuum being used as an auxiliary tool. To study discrete traveling waves, instead of a direct study of the waveform, we position ourselves at a given point and follow the time, which is a continuous variable, as the wave passes the observer. To this end we make the traveling wave ansatz $v_n(t) = v(t - bn)$ where $b = 1/\lambda$ is the inverse velocity. Positing it in (7) we obtain a delay-advanced equation

$$\dot{v} = q[v(t - b)] - q[v(t + b)]. \tag{37}$$

Integration of (37) yields

$$v(t) = \int_{t-b}^{t+b} [q(0) - q(v(s))]\mathrm{d}s. \tag{38}$$

The choice of the integration constant ensures that $v = 0$ is a solution.

Note that since Eqs. (37) and (38) have no singularities, rather than to use constant state solutions $v = v_*$ where $q'(v_*) = 0$, we may attempt solutions with an arbitrary v^*. It follows then from (38) that for such a solution to exist we need that the corresponding speed satisfies

$$\lambda^* = 2\frac{q(0) - q(v^*)}{v^*}. \tag{39}$$

Remarkably, this condition is exactly analogous to condition (23) imposed in quasicontinuum for the force to vanish at the singular point. To obtain an analog of condition (28) we integrate (38) (assuming $b = \frac{1}{\lambda^{**}}$) and obtain

$$\int_{-\infty}^{\infty} \left[v(t) - \frac{2}{\lambda^{**}}\{q(0) - q(v(t))\} \right] \mathrm{d}t = 0. \tag{40}$$

However, this condition is not very practical as one has to know the sought-after solution $v(t)$. Nevertheless, when q is symmetric $q(v) + q(v^* - v) = q(0) + q(v^*)$, assuming that the solution is also symmetric: $v(-t) + v(t) = v^*$, then for $\lambda^{**} = \lambda^*$ the function to be integrated in (40) is odd and the integral vanishes. Thus condition (40) is automatically satisfied. In particular, this symmetry implies (29) and holds for $q(v) = \cos v$. Thus what in PDEs was accomplished directly via symmetries and singularity, is also embedded in the discrete antecedent albeit in a more implicit way. The present discussion makes it also clear that a more general coupling function q may lead to asymmetric solutions. This issue will be explored elsewhere.

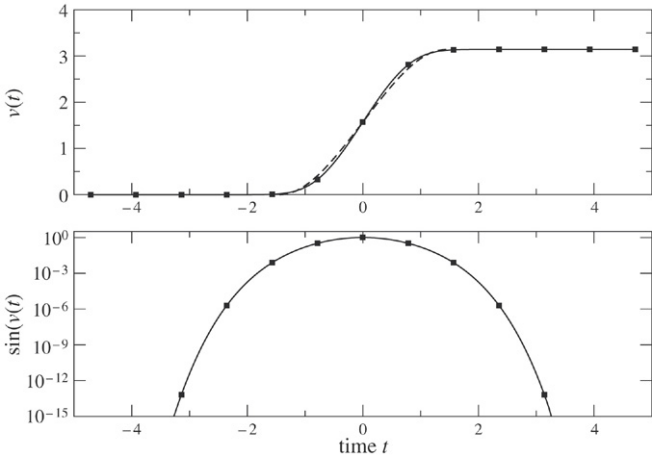

Fig. 2. Top panel: the form of the kink traveling wave. Bottom panel: the kink in logarithmic scale. The function $\sin(v(t))$ is plotted to reveal the approach to asymptotic values both at $v = 0$ and $v = \pi$. Markers show the kink on the discrete lattice. The dashed line is the corresponding solution in the quasicontinuum approximation.

From now on we shall be concerned with the $q(v) = \cos v$ case, where the homogeneous states of interest are $v = 0$ and $v^* = \pi$. The latter state, according to the preceding discussion, is a solution for $\lambda^* = 4/\pi$ only. Notice also that $\lambda^* = \lambda_* = \lambda_c$. To find the form of a kink connecting the two homogeneous states we solve Eq. (38) for $b = \pi/4$ using a simple iterative process that converges to the solution:

$$v_{k+1}(t) = \int_{t-\pi/4}^{t+\pi/4} [1 - \cos v_k(x)]\mathrm{d}x \tag{41}$$

(k is the iteration step). We initially guess $v_0(x)$ and use a high-order Lagrangian integration rule [45]. The resulting solution is presented in Fig. 2.

To find the profile of the compacton we had to modify the direct iterative process because a convergence to a trivial solution may occur. A similar improved iterative method was already proposed by Petviashvili [46,47]. We thus iterate

$$\tilde{v}(t) = \int_{t-b}^{t+b} (1 - \cos v_k(x))\mathrm{d}x, \quad v_{k+1} = \left(\frac{\|v_k\|}{\|\tilde{v}\|}\right)^{3/2} \tilde{v}, \tag{42}$$

(the L_1-norm is used). The results for $b = 1$ are displayed in Fig. 3. Using (41) and (42) we were able to determine numerically traveling waves in the whole range of velocities $0 < \lambda \leq \lambda_c$.

4.3. Estimate of the tails

Though, clearly, the integral equation for the traveling wave (38) does not support truly compact solutions, it enables us to estimate the decay rate of the tails (see [48] for a similar analysis for waves in a chain of elastic spheres). For small v we

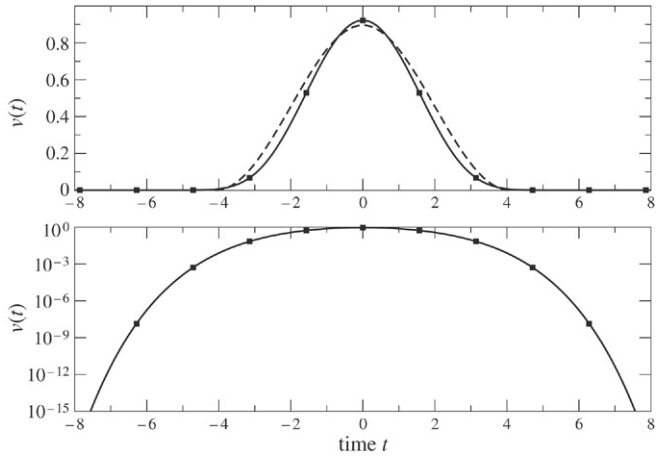

Fig. 3. Top panel: the form of the localized traveling wave for $\lambda = 0.5\lambda_c = 2/\pi$. Bottom panel: the same in logarithmic scale. Markers show the wave form on the discrete lattice. The dashed line represents the corresponding solution in the quasicontinuum approximation.

can rewrite it as

$$v(t) = \int_{t-b}^{t+b} v^2(\tau)\mathrm{d}\tau. \tag{43}$$

We assume that $v(t) \sim \mathrm{e}^{-f(t)}$ and that for large t, $f(t)$ is a rapidly growing function. Then we follow Watson's Lemma procedure to estimate the integral

$$v(t) \approx \mathrm{e}^{-2f(t-b)} \frac{1}{2f'(t-b)}. \tag{44}$$

We rewrite (44) as

$$\mathrm{e}^{-f(t)} = \mathrm{e}^{-2f(t-b)} \frac{1}{2f'(t-b)}$$

or as

$$f(t) = 2f(t-b) + \ln 2f'(t-b). \tag{45}$$

In the first approximation we neglect the logarithmic term and obtain $f_0(t) = 2f_0(t-b)$ with a solution $f_0(t) = C2^{t/b} = C\exp(\frac{\ln 2}{b}t)$ where C is an arbitrary constant. For the first correction $f_1(t)$ we obtain from (45)

$$f_1(t) - 2f_1(t-b) = \ln 2 f_0'(t-b) = \ln C \frac{\ln 2}{b} + \frac{\ln 2}{b} t.$$

Seeking a solution of the form $f_1(t) = At + B$ we obtain

$$At + B - 2A(t-b) - 2B = +\ln C \frac{\ln 2}{b} + \frac{\ln 2}{b} t.$$

Thus

$$A = -\frac{\ln 2}{b} \quad B = -2\ln 2 - \ln C \frac{\ln 2}{b} = \ln \frac{b}{C4\ln 2},$$

which finally yields

$$f(t) = C\exp\left(\frac{\ln 2}{b}t\right) - t\frac{\ln 2}{b} + \ln \frac{b}{C4\ln 2}.$$

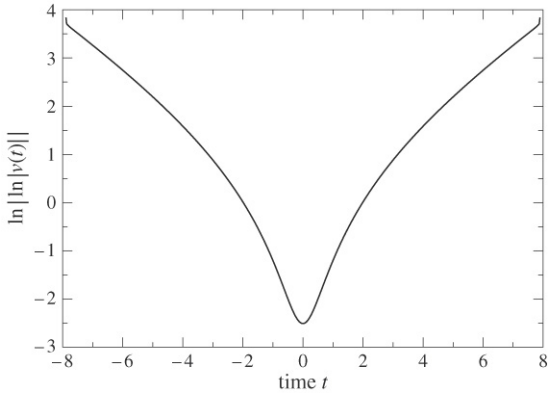

Fig. 4. The compacton Fig. 3 in a doubly logarithmic scale. The nearly linear tails are consistent with estimate (46).

For large t we may neglect the last term and obtain

$$v \approx \mathrm{e}^{-f(t)} = \exp\left[-C\exp\left(\frac{\ln 2}{b}t\right) + t\frac{\ln 2}{b}\right]. \tag{46}$$

The superexponential decay of tails is visualized in Fig. 4 where the compacton of Fig. 3 is presented on a doubly logarithmic scale.

Perhaps the most remarkable feature of our analysis is the fact that the structures obtained on the basis of quasicontinuum, which appends the continuum with a leading dispersive effect, *approximate so well the exact discrete process*. One expects quasicontinuum to approximate well a dense lattice which is close to continuum, but our lattice is sparse. The main core of the discrete solution consists of five points, and 2–3 points at each side of the tail. Any point beyond has no measurable effect. Part of the explanation for the remarkable proximity can be attributed to $q(v)$ being a symmetric function, with the global conditions for the lattice and quasicontinuum being the same and automatically satisfied.

5. Numerical studies

In this section we describe numerical simulations of the lattice (7). We do not aim to provide a comprehensive classifications of all possible regimes, rather we dwell on the features that we find notable, if not remarkable. We start with long chains (effectively infinite chains) so that boundary effects are irrelevant and in Section 6 we shall present the long-time behavior in finite lattices.

5.1. Evolution from a compact initial datum

Initial conditions are taken in a form of an unimodal pulse

$$v_n(0) = A\sin\left(\pi\frac{n-n_0}{M}\right), \tag{47}$$

with two free parameters — amplitude A and width M. From Fig. 5(a) one notes that a relatively wide pulse decomposes into a sequence of compactons. The adjective 'wide' means that the pulse's width is many time that of the compacton. That the emerging compactons are ordered according to their

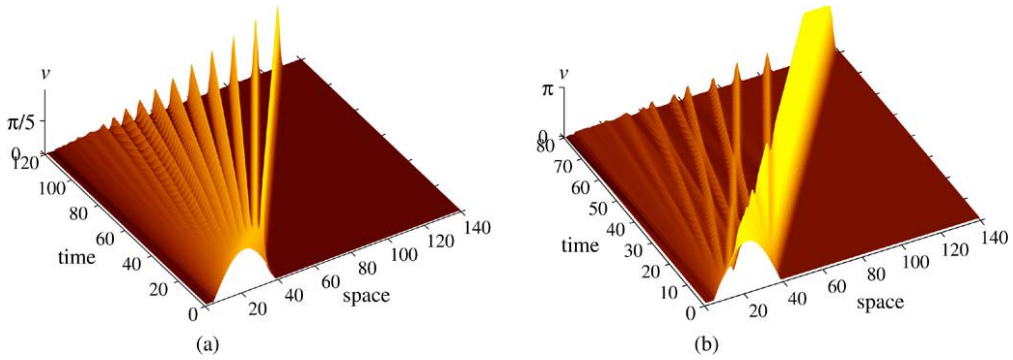

Fig. 5. Evolution of the initial pulse (47). (a): $M = 34$, $A = \pi/4$ (b): $M = 34$, $A = \pi$.

amplitudes is natural because their velocities are monotonously related to their amplitudes, see (35). In addition to compactons, an initial pulse of a larger amplitude produces a new object – *kovaton* – which we have seen in the quasicontinuum, and is a composition of two kinks propagating with the same critical velocity λ_c, see Fig. 5(b). In this simulation two features are to be noted:

(i) The number of the emitted compactons decreases.
(ii) Though an increase in the amplitude may widen the emerging kovaton, a natural way to induce wider kovatons is to start with a wider initial condition.

To obtain some quantitative feeling, we characterize in Fig. 6 the dependence of the emitted objects on the parameters of the initial pulse. Here the initial pulse is given via (47) with a fixed width $M = 34$ and a varying amplitude A. In Fig. 6 the amplitudes of emitted compactons are presented. When $A < \pi/2$ only compactons emerge, while for larger amplitudes a kovaton (in this representation it is a 'limiting compacton with an amplitude π') appears. Notably, for $A > 3\pi/4$ some compactons appear 'in pairs'. A detailed inspection of space-time plots like Fig. 5b shows that these compactons appear nearly symmetrically at the left and right edges of the initial pulse. Almost all compactons have positive amplitudes and propagate to the right, however, for $A > \pi/4$ there is at least one compacton propagating to the left.

When the initial profile is relatively narrow, apart from a kovaton and a number of compactons, it also generates a standing source of waves. An example of such structure is depicted in Figs. 7 and 8. At this point we lack a theoretical explanation for this wave source.

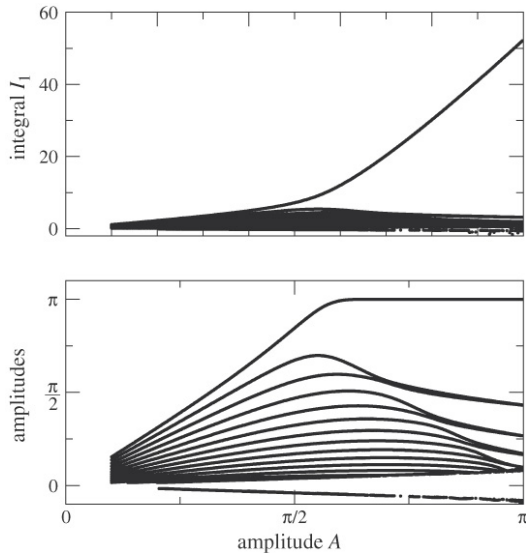

Fig. 6. Compactons and a kovaton resulting from the initial profile (47) with $M = 34$ and different initial amplitudes A. Upper panel: values of integral I_1 (11); bottom panel: the amplitude. The kovaton first appears at $A \approx \pi/2$, its amplitude is constant but the width and, correspondingly, the value of I_1, increase with A. Since the small-amplitude compactons evolve very slowly, a finite time integration probably will miss some of these compactons.

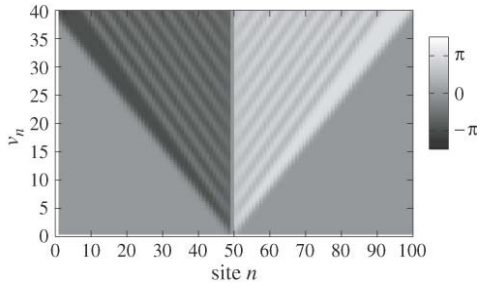

Fig. 7. Evolution of an initial field $v_k(0) = -1$, $v_{k+1} = 1$, and $v_n = 0$ for all other n. See also Fig. 8. The leading edge is formed by a $0 - \pi$ kink, the width of the plateau at $u = \pi$ is growing along the propagation front.

5.2. *Collisions of compactons and kovatons*

We start with a collision of two compactons in Fig. 9. Discrete compactons are robust, but the collision is not entirely elastic, as may be read from Fig. 10, where we depict the maximal value of the field at each site. In the collision region these maxima are not the amplitudes of the compactons, but outside of it they are. The initial amplitudes of the compactons are 0.27595 and 1.3955. After the collision the measured amplitude of the larger compacton was 1.3956, the amplitude of the smaller one varied in the range 0.27407–0.27411 depending on the initial separation of compactons. The amplitude losses of the smaller compacton are more significant. After the collision the collision site is marked with a left over residuum that decomposes very slowly into small-amplitude pairs of anti-compactons that are emitted to the left and compactons that are emitted to the right. In Fig. 11 we show the amplitudes of the emitted compactons and the characteristic times at which

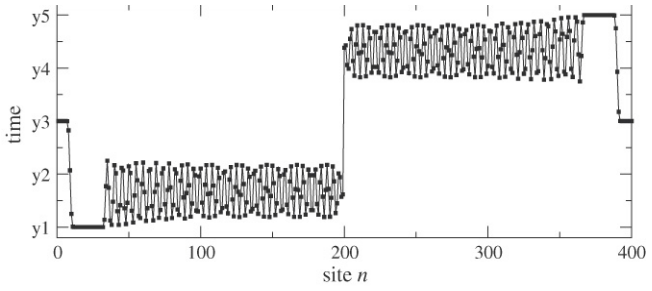

Fig. 8. The final waveform at $t = 150$ for the same initial conditions as in Fig. 7. Two symmetric kovatons (or, if one desires, a kovaton and an antikovaton) are followed by propagating waves.

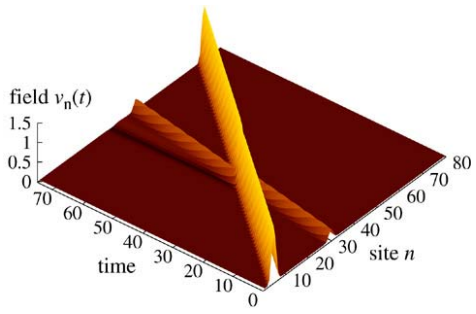

Fig. 9. Collision of two compactons having velocities 0.2 and 0.9.

they leave the collision domain. This process may, presumably, continue indefinitely. Note that at small amplitudes the process is invariant under scaling (19). Thus it takes 'forever' for the smaller compactons to emerge.

In Fig. 12 we show a symmetric collision of a compacton and an anticompacton (both have speed 0.5). Remarkably, while both compactons survive the collision, a pair of larger compactons is born. This can be attributed to the small amplitude instability mentioned in Section 3.2.

Next, in Fig. 13 we consider a collision of a compacton and a kovaton. The features of this collision are similar to that of two compactons: the amplitude of the compacton decreases slightly after collision (for the displayed case from 0.560164 to 0.556288) with some leftover marking the collision site. The kovaton also experienced small changes: its integral I_1 (Eq. (11)) increased from 31.4159 to 31.4167. Finally, in Fig. 14 we illustrate a collision of a kovaton with an antikovaton. Both objects preserve their amplitude after the collision, but a ripple emerges.

5.3. Interpretation of solutions in terms of oscillators phases

So far we have considered the solutions of the lattice (8) in terms of the derived field variable $v_n(t)$. We now return to the original phases. According to (3), the oscillator phase is $\varphi_n = \sum^n v_k$. Thus compacton solution of $v_n(t)$ corresponds to a propagating step between two domains of constant phases. We illustrate this field in Fig. 15, which corresponds to the solution of Fig. 5(a).

Lattice with $v_n = 0$ is in-phase, while for $v_n = \pi$ the neighboring states are in anti-phase, with the differences between the oscillator phases being now π. Thus a kink $0 - \pi$ shown in Fig. 2 is an interface moving between the in-phase and anti-phase states. A kovaton is a segment of a lattice in the anti-phase state which propagates within an in-phase lattice. The one in Fig. 16 corresponds to the solution in Fig. 5(b).

6. Chaos in a finite lattice

6.1. Equations for finite lattices

So far we have considered an infinite lattice of coupled oscillators. In a finite lattice we have to append the problem with suitable boundary conditions. We restrict our attention to oscillator lattices of finite length N with 'open ends'. Eq. (2) are then valid in the bulk while the first and last oscillator are driven by one neighbour only

$$\dot\varphi_1 = q(\phi_2 - \phi_1), \qquad \dot\varphi_N = q(\phi_{N-1} - \phi_N). \tag{48}$$

Consequently, the equations for v_1 and v_{N-1} have to be modified and instead of (7) we have

$$\begin{aligned} \dot v_1 &= q(v_2), \\ \dot v_n &= q(v_{n+1}) - q(v_{n-1}) \quad 2 \le n \le N-2, \\ \dot v_{N-1} &= -q(v_{N-2}). \end{aligned} \tag{49}$$

These boundary conditions are important for spatially homogeneous states. The state with $v_n = V$ is possible only if $q(V) = 0$. Thus if $q(v) = \cos v - 1$, then the in-phase state $v = 0$ exists but the anti-phase state $v = \pi$ does not. Also the conservation laws (11)–(13) have to be reconsidered. Property

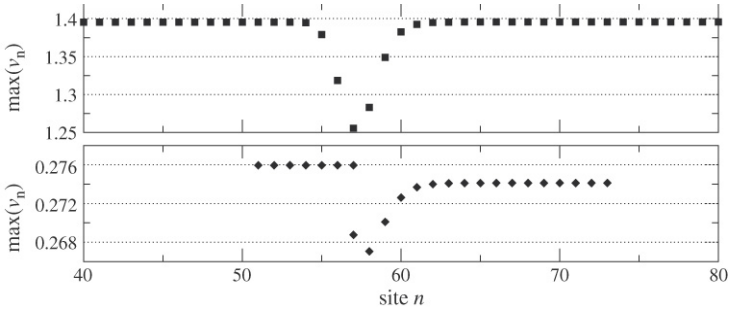

Fig. 10. Maxima of the field at different sites for the collision Fig. 9. Upper panel shows the values for the larger compacton, bottom panel for the smaller one. Both compactons propagate from left to right.

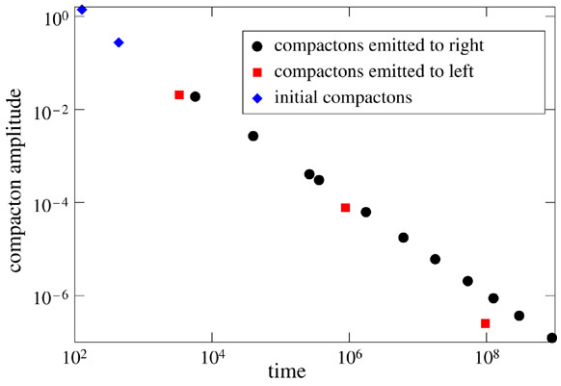

Fig. 11. Amplitudes of compactons evolving from a ripple left after the collision Fig. 9. Compactons evolve to the right and anticompactons, far fewer, to the left. This, due to mass conservation, is a reflection of the fact that the total mass of the ripple was not zero, i.e., some mass was lost during the collision of compactons.

(13) is valid for any N, while a combination of I_1 and I_2 is for even N's only. Thus the finite lattice (49) conserves

$$S = \sum_{n=1}^{N-1} Q(v_n), \quad \text{and} \quad K = \sum_{n=1}^{\left[\frac{N}{2}\right]} v_{2n-1} \quad (\text{for even } N). \tag{50}$$

Remarkably, system (49) is Hamiltonian[2]: for even $N = 2m+2$ one has

$$H = Q(s_1) + \sum_{n=1}^{m} Q(p_n) + \sum_{n=1}^{m-1} Q(s_{n+1} - s_n) + Q(K - s_n), \tag{51}$$

while for odd $N = 2m + 1$, the Hamiltonian is

$$H = Q(s_1) + \sum_{n=1}^{m} Q(p_n) + \sum_{n=1}^{m-1} Q(s_{n+1} - s_n). \tag{52}$$

Canonical variables $\{s_n, p_n\}$ are then defined according to

$$p_n = v_{2n}, \quad s_n = \sum_{j=1}^{n} v_{2j-1}. \tag{53}$$

Note that the integral S is the 'energy' and the unusual form of the kinetic energy $Q(P)$.

6.2. Destruction of compactons and the emergence of chaos

In Fig. 17 we show what happens to an initial compacton (having velocity $\lambda = 0.7$) in a lattice with boundary conditions (49) and $q(v) = \cos v - 1$: after a few 'reflections' from the boundaries the compact structure is lost and an irregular regime emerges.

To study whether regular or chaotic regimes are predominant in the lattice (49) we carried out statistical tests: starting with randomly chosen initial conditions we calculated the Lyapunov exponents. The results are presented in Fig. 18. We used lattices

[2] This observation is due to Holger Dullin.

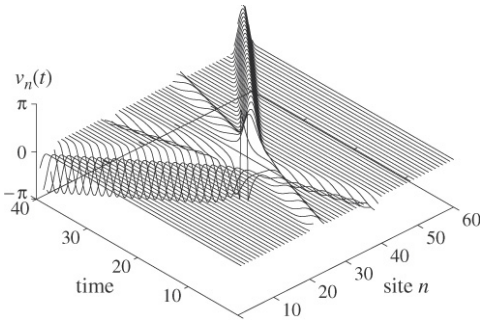

Fig. 12. Collision of a compacton and an anticompacton gives rise to a pair of large-amplitude compactons.

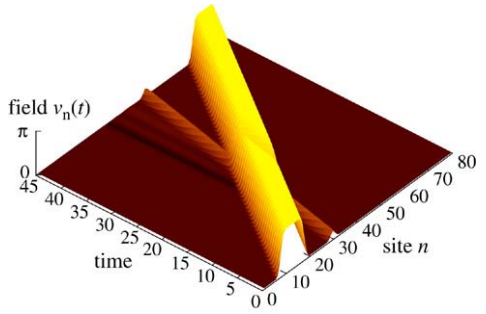

Fig. 13. Collision of kovaton ($\lambda = 4/\pi$) with compacton ($\lambda = 0.4$).

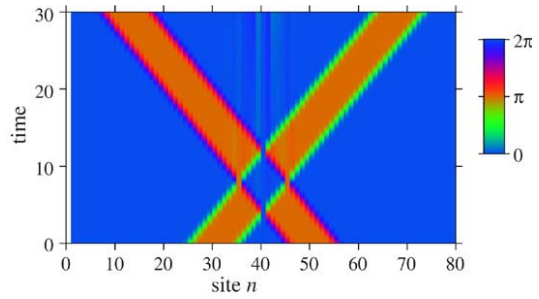

Fig. 14. Collision of a kovaton with an antikovaton. Unlike Figs. 12 and 13, we do not present the data as a surface plot like in Figs. 12 and 13 because the field profile taken modulo 2π looks rather erratic, because if at certain lattice sites the field v rotates by values larger than $\pm 2\pi$, then after remapping it to the $(0, 2\pi)$ interval, one obtains vertical lines corresponding to 2π-jumps. Such jumps can be already seen in Fig. 12; for the processes presented in this figure and Figs. 15–17 below the number of these jumps is even larger. Therefore, instead of drawing a surface, we use here a color coding that is 2π-periodic (a corresponding continuous gray coding is impossible).

of length $N = 5$ and $N = 7$, because for these odd N's only one integral exist. These are Hamiltonian systems with two and three degrees of freedom, respectively. Remarkably, a regular behavior appears to be rather improbable. For $N = 5$ almost always a chaotic dynamics with one positive Lyapunov exponent has been observed, only 6 runs out of 3000 yielded zero Lyapunov exponents. For $N = 7$ in all 3000 numerical runs only two positive Lyapunov exponents have been observed.

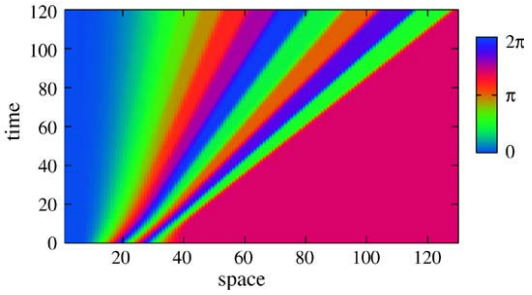

Fig. 15. The phase field corresponding to the solution Fig. 5(a), in the same color coding as in Fig. 14. The initial profile (47) corresponds to the phase step. This step evolves into a number of smaller steps corresponding to compactons. Between these steps the phase is constant (stripes of uniform color).

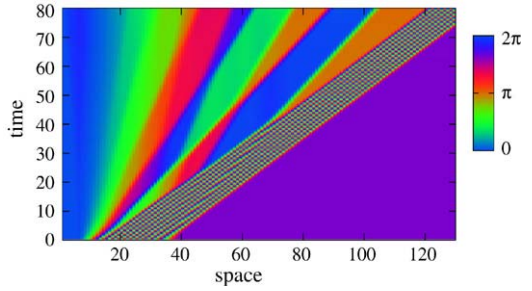

Fig. 16. The phase field corresponding to the solution in Fig. 5(b), it has the same color coding as Fig. 14. The initial profile (47) corresponds to the phase step. This step evolves into a number of smaller steps represented by compactons. Between these steps the phase is constant. The kovaton in this picture appears as a chessboard strip: a segment of the anti-phase state propagating over the in-phase state.

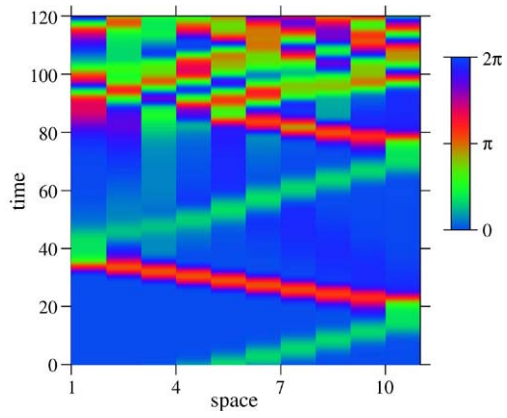

Fig. 17. Evolution of the initial compacton with $\lambda = 0.7$ in a lattice of $N = 11$ oscillators (10 values of v_n are shown in the same color coding as in Fig. 14).

For large N a spectrum of Lyapunov exponents is observed, [49]. Plotted as functions of the number normalized by N, they form a universal curve (Fig. 19) which is typical for spatio-temporal chaos. Notably, in all our calculations the number of zero Lyapunov exponents was two for odd N's and three for even N's, which clearly demonstrates that there are no additional integrals beyond the aforementioned ones S and K.

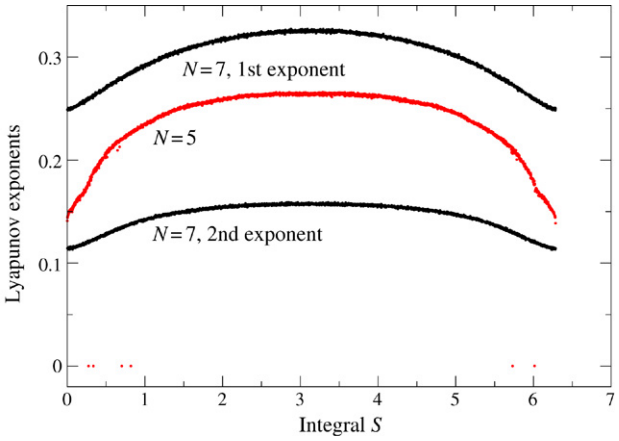

Fig. 18. Lyapunov exponents in dependence on the integral S for lattices of length $N = 5$ and $N = 7$.

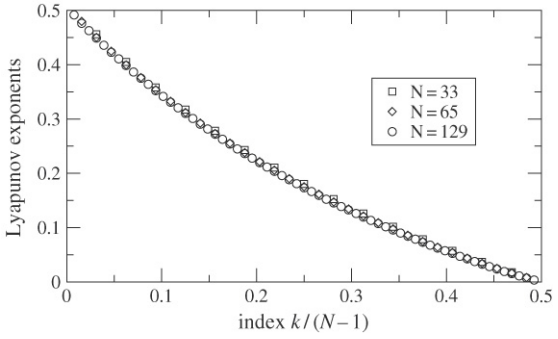

Fig. 19. Spectra of Lyapunov exponents for $N = 33, 65, 129$ for $S = 0$: Lyapunov exponents Λ_k are drawn in dependence on the normalized index $k/(N-1)$. The curves converge to an asymptotic Lyapunov spectrum; only the positive part of spectrum is shown, the negative part is symmetric to it.

7. Complex Ginzburg–Landau lattice

In this section we demonstrate how realistic dispersively coupled oscillators give rise to phase equations similar to the ones discussed above plus some dissipative effects.

7.1. Complex Ginzburg–Landau lattice

The celebrated complex Ginzburg–Landau equation describes spatio-temporal dynamics in an active medium close to a Hopf bifurcation [49,50]. Its version on a lattice, the Complex Ginzburg–Landau Lattice (CGLL),

$$\frac{\mathrm{d}A_n}{\mathrm{d}t} = A_n(1-(1+ic_1)|A_n|^2) + (c_2+ic_3) \times (A_{n-1}+A_{n+1}-2A_n), \tag{54}$$

describes a chain of self-sustained oscillators with a linear coupling. Here time and the complex amplitude A_n are normalized so that the stationary amplitude of a single oscillator is $|A_n| = 1$ and its linear growth rate is unity. Parameter c_1 characterizes a nonisochrony of a single oscillator, while c_2 and c_3 represent the dissipative and reactive parts of the coupling, respectively. Considering the coupling parameters as small, we

reduce (see details in the Appendix) the dynamics to a phase equation

$$\dot{v}_n = (c_3 - c_1c_2)\nabla_d \cos v + (c_2 + c_1c_3)\Delta_d \sin v + \frac{c_2^2}{2}\nabla_d(\sin v \nabla_d \cos v) + \frac{c_2c_3}{2}\Delta_d(\cos v \nabla_d \cos v) - \frac{c_2c_3}{2}\Delta_d(\sin v \Delta_d \sin v) - \frac{c_3^2}{2}\Delta_d(\cos v \Delta_d \sin v). \quad (55)$$

This equation contains both terms linear in coupling ($\propto c_2, c_3$) and quadratic ones. For isochronous oscillators with $c_1 = 0$ the first order c_3-term is dispersive and corresponds to even coupling of phases while the c_2-term is dissipative (odd coupling function). In the second order in coupling it is not so easy to classify the higher order operators.

In Fig. 20 we illustrate the evolution of a compacton in the CGLL, Eq. (54). As an initial condition we have used a compacton solution of (8) with velocity $\lambda = 0.5$. Coupling parameters were fixed at $c_2 = 0$, $c_3 = 0.01$ and the nonisochronicity parameter of the single oscillator, c_1, was varied. For this choice of parameters (55) reduces to

$$\frac{1}{c_3}\frac{\mathrm{d}v_n}{\mathrm{d}t} = \nabla_d \cos v + c_1\Delta_d \sin v - \frac{c_3}{2}\Delta_d(\cos v \Delta_d \sin v). \quad (56)$$

Eq. (56) has two dissipative parts. For states with nearly uniform phase, i.e. for $v \approx 0$, the third term is dissipative. The nature of the second term depends on the sign of c_1 and is anti-dissipative for $c_1 < 0$. For large $|c_1|$ the second term prevails,[3] which means that the anti-phase state is more stable than the in-phase state. However, this changes for small $|c_1|$. Accordingly, one observes an acceleration and growth of the amplitude of the compacton for large $|c_1|$, and deceleration and decrease in amplitude for small $|c_1|$. For the particular compacton in Fig. 20 with $c_1 \approx -0.0065$ the two opposing effects nearly cancel and the compacton propagates at an almost constant velocity.

7.2. Perturbation theory for compactons

In this section we develop a simple perturbation theory for small-amplitude compactons and use the quasicontinuum approximation of Section 3.3 with the compacton given by Eq. (32).

Inspecting Eq. (55) we note that for small v's, except for the leading first term, only the second and the last terms on the r.h.s. are important. Thus for small-amplitude compactons we write a small-amplitude variant of (56)

$$\dot{v}_n = -\frac{1}{2}\nabla_d v^2 + \alpha\Delta_d v + \beta\Delta_d^2 v, \quad (57)$$

which on the quasicontinuum level yields

$$\frac{\partial v}{\partial t} = -\left(\frac{\partial}{\partial x} + \frac{1}{6}\frac{\partial^3}{\partial x^3}\right)v^2 + \alpha\frac{\partial^2}{\partial x^2}v + \beta\frac{\partial^4}{\partial x^4}v. \quad (58)$$

[3] Note, however, that a direct comparison of the two dissipative effects is a bit tricky because, using in continuum limit the second term on the r.h.s. of (56) turns into a Laplacian Δ_d while the third term into a bi-Laplacian Δ_d^2. Each of these operators has its particular properties (the bi-Laplacian does not, for instance, preserve the maximum principle and initially positive data need not remain so).

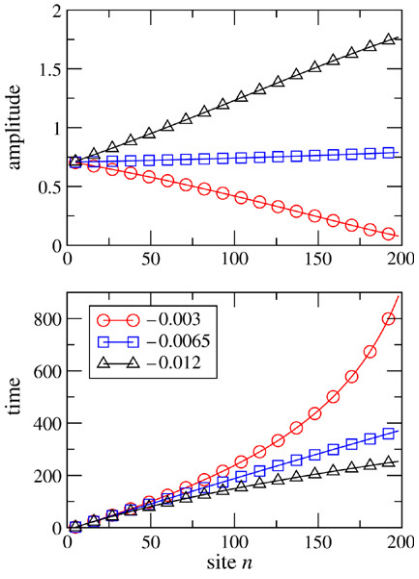

Fig. 20. Amplitude (top panel) and space-time trajectory (bottom panel) of a propagating compacton (with $\lambda = 0.5$) for three values of constant c_1 for the complex Ginzburg–Landau lattice (54) with $c_2 = 0$, $c_3 = 0.01$.

We use the integrals of the unperturbed (i.e. with $\alpha = \beta = 0$) version of (58) (cf. (11) and (13)) $I_1 = \int_{-\infty}^{\infty}\mathrm{d}x\, v$ and $I_3 = \int_{-\infty}^{\infty}\mathrm{d}x\, v^3$ to find the evolution of the compacton (32): $v_c(x,t) = \frac{4\lambda}{3}\cos^2 k(x - \lambda t)$ where $k = \sqrt{3/8}$. Writing an equation for the evolution of I_3 we have

$$\frac{\mathrm{d}}{\mathrm{d}t}\int_{-\pi/2k}^{\pi/2k}\mathrm{d}x\, v_c^3 = 3\int_{-\pi/2k}^{\pi/2k}\mathrm{d}x\, v_c^2\left(\alpha\frac{\partial^2}{\partial x^2} + \beta\frac{\partial^4}{\partial x^4}\right)v_c. \quad (59)$$

Evaluation of the integrals yields

$$\frac{\mathrm{d}\lambda}{\mathrm{d}t} = -\frac{3}{5}\left(\alpha - \frac{3}{2}\beta\right)\lambda. \quad (60)$$

Since the integral I_1 is conserved in the presence of perturbations (58), this allows us to find the 'tail' that appears due to changes in the compacton's amplitude. First, we write the conservation of I_1 as

$$\int \mathrm{d}x\, v_c(x,t) + \int \mathrm{d}x\, v_{\mathrm{tail}}(x,t) = I_1 = \mathrm{const}. \quad (61)$$

Now suppose that the tail stretches from the initial position of the compacton $x = 0$ up to its present position $X = \int_0^t \lambda(\tau)\mathrm{d}\tau$. Then from (60) and (61)

$$\frac{\mathrm{d}}{\mathrm{d}X}\int_0^X \mathrm{d}x\, v_{\mathrm{tail}}(x,t) = -\frac{1}{\lambda}\frac{\mathrm{d}}{\mathrm{d}t}\int \mathrm{d}x\, v_c(x,t) = \frac{2\pi}{5k}\left(\alpha - \frac{3}{2}\beta\right). \quad (62)$$

This means that the tail has a constant plateau

$$v_{\mathrm{tail}} = \frac{2\pi}{5k}\left(\alpha - \frac{3}{2}\beta\right). \quad (63)$$

This plateau is positive if the compacton decays and negative if it grows. Estimates (60) and (63) are in good agreement with numerics.

8. Conclusions

In this paper we have demonstrated that in lattices of dispersively coupled autonomous, self-sustained oscillators, compactons and kovatons are the natural building blocks of the dynamics. In a lattice these nonlinear solitary waves with an almost-compact support are possible thanks to a degeneracy of the linearized part resulting, in particular, in a nonexistence of linear waves. Remarkably, the phase dynamics of oscillator lattices is a physically observable phenomenon because the phase space of a finite lattice is a torus, thus the solutions are well-defined at all times. Numerics shows, however, that compactons and kovatons, although undergoing almost elastic collisions, on a long time scale induce a spatio-temporal chaos.

It is clear that in spite of the volume of this article, many interesting and important issues concerned with the phase dynamics of compacton-bearing lattices are yet to be addressed. This is left for a forthcoming work.

Acknowledgements

We thank H. Dullin, Y. Kuramoto, M. Rosenblum and S. Schochet for useful discussions. The work of PR was supported in part through the Alexander von Humboldt award and in part via the DFG (Sonderforschungsbereich 555 Complex Nonlinear Processes).

Appendix. The complex Ginzburg–Landau lattice

Let $A_k = R_k e^{i\varphi_k}$, then (54) can be written as

$$\begin{aligned}
\dot{R}_k &= r_k - R_k^3 + c_2(R_{k+1}\cos(\varphi_{k+1}-\varphi_k) \\
&\quad + R_{k-1}\cos(\varphi_{k-1}-\varphi_k) - 2R_k) \\
&\quad - c_3(R_{k+1}\sin(\varphi_{k+1}-\varphi_k) \\
&\quad + R_{k-1}\sin(\varphi_{k-1}-\varphi_k)), \\
\dot{\varphi}_k &= -c_1 R_k^2 + c_2\left(\frac{R_{k+1}}{R_k}\sin(\varphi_{k+1}-\varphi_k)\right. \\
&\quad \left. + \frac{R_{k-1}}{R_k}\sin(\varphi_{k-1}-\varphi_k)\right) + c_3\left(\frac{R_{k+1}}{R_k}\cos(\varphi_{k+1}-\varphi_k)\right. \\
&\quad \left. + \frac{R_{k-1}}{R_k}\cos(\varphi_{k-1}-\varphi_k) - 2\right).
\end{aligned}$$

We now expand in small parameters c_2 and c_3.

In the 'zeroth' order a limit cycle with $R = 1$ sets on. In the next order we take $R = 1 + r$ and introduce a new variable $v_k = \varphi_{k+1} - \varphi_k$. Thus

$$\begin{aligned}
\dot{r}_k &= -2r_k + c_2(\cos(v_k) + \cos(v_{k-1}) - 2) \\
&\quad - c_3(\sin(v_k) - \sin(v_{k-1})).
\end{aligned}$$

As the amplitude follows the variations of the phases, we assume that $\dot{r}_k \approx 0$ and obtain

$$r_k = \frac{c_2}{2}(\cos(v_k) + \cos(v_{k-1}) - 2) - \frac{c_3}{2}(\sin(v_k) - \sin(v_{k-1})),$$

to be used in the equation for φ_k, but first:

$$\begin{aligned}
R_k^2 &\approx 1 + 2r_k, \\
\frac{R_{k+1}}{R_k} &\approx 1 + r_{k+1} - r_k = 1 + \frac{c_2}{2}\nabla_d \cos v_k - \frac{c_3}{2}\Delta_d \sin v_k, \\
\frac{R_{k-1}}{R_k} &\approx 1 + r_{k-1} - r_k = 1 - \frac{c_2}{2}\nabla_d \cos v_{k-1} + \frac{c_3}{2}\Delta_d \sin v_{k-1}.
\end{aligned}$$

This gives

$$\begin{aligned}
\dot{\varphi}_k &= -c_1 - c_1c_2(\cos v_k + \cos v_{k-1} - 2) \\
&\quad + c_1c_3(\sin v_k - \sin v_{k-1}) \\
&\quad + c_2(\sin v_k - \sin v_{k-1}) + c_3(\cos v_k + \cos v_{k-1}) \\
&\quad + (c_2 \sin v_k + c_3 \cos v_k)\left(\frac{c_2}{2}\nabla_d \cos v_k - \frac{c_3}{2}\Delta_d \sin v_k\right) \\
&\quad - (c_2 \sin v_{k-1} - c_3 \cos v_{k-1})\left(-\frac{c_2}{2}\nabla_d \cos v_{k-1}\right. \\
&\quad \left. + \frac{c_3}{2}\Delta_d \sin v_{k-1}\right).
\end{aligned}$$

Finally, composing an equation for phase differences v_k we obtain

$$\begin{aligned}
\dot{v}_k &= (c_3 - c_1c_2)\nabla_d \cos v_k + (c_2 + c_1c_3)\Delta_d \sin v_k \\
&\quad + \frac{c_2^2}{2}\nabla_d(\sin v_k \nabla_d \cos v_k) + \frac{c_2c_3}{2}\Delta_d(\cos v_k \nabla_d \cos v_k) \\
&\quad - \frac{c_2c_3}{2}\Delta_d(\sin v_k \Delta_d \sin v_k) - \frac{c_3^2}{2}(\cos v_k \Delta_d \sin v_k).
\end{aligned}$$

As in (10), in the first order in c_2, c_3 only the first two terms appear.

References

[1] Ch. Huygens, Horologium Oscillatorium, Apud F. Muguet, Parisiis, France, 1673, English translation: The Pendulum Clock, Iowa State University Press, Ames, 1986.
[2] E.V. Appleton, The automatic synchronization of triode oscillator, Proc. Camb. Phil. Soc. (Math. and Phys. Sci.) 21 (1922) 231–248.
[3] L. Glass, Synchronization and rhythmic processes in physiology, Nature 410 (2001) 277–284.
[4] A. Pikovsky, M. Rosenblum, J. Kurths, Synchronization, in: A Universal Concept in Nonlinear Sciences, Cambridge University Press, Cambridge, 2001.
[5] Y. Kuramoto, Chemical Oscillations, Waves and Turbulence, Springer, Berlin, 1984.
[6] R. Adler, A study of locking phenomena in oscillators, Proc. IRE 34 (1946) 351–357. Reprinted in. Proc. IEEE 61 (10) (1973) 1380–1385.
[7] G.B. Ermentrout, N. Kopell, Frequency plateaus in a chain of weakly coupled oscillators, I, SIAM J. Math. Anal. 15 (2) (1984) 215–237.
[8] N. Kopell, G.B. Ermentrout, Symmetry and phase locking in chains of weakly coupled oscillators, Comm. Pure Appl. Math. 39 (1986) 623–660.
[9] H. Sakaguchi, S. Shinomoto, Y. Kuramoto, Mutual entrainment in oscillator lattices with nonvariational type interaction, Prog. Theor. Phys. 79 (5) (1988) 1069–1079.
[10] L. Ren, B. Ermentrout, Phase locking in chains of multiple-coupled oscillators, Physica D 143 (1–4) (2000) 56–73.
[11] D. Topaj, A. Pikovsky, Reversibility versus synchronization in oscillator lattices, Physica D 170 (2) (2002) 118–130.
[12] Y. Kuramoto, Self-entrainment of a population of coupled nonlinear oscillators, in: H. Araki (Ed.), International Symposium on Mathematical Problems in Theoretical Physics, in: Lecture Notes Phys., vol. 39, Springer, New York, 1975, p. 420.

[13] H. Daido, Order function and macroscopic mutual entrainment in uniformly coupled limit-cycle oscillators, Prog. Theor. Phys. 88 (6) (1992) 1213–1218.
[14] H. Daido, Quasientrainment and slow relaxation in a population of oscillators with random and frustrated interactions, Phys. Rev. Lett. 68 (7) (1992) 1073–1076.
[15] S.H. Strogatz, From Kuramoto to Crawford: Exploring the onset of synchronization in populations of coupled oscillators, Physica D 143 (1–4) (2000) 1–20.
[16] K.Y. Tsang, R.E. Mirollo, S.H. Strogatz, K. Wiesenfeld, Dynamics of globally coupled oscillator array, Physica D 48 (1991) 102–112.
[17] S. Nichols, K. Wiesenfeld, Ubiquitous neutral stability of splay-phase states, Phys. Rev. A 45 (1992) 8430–8435.
[18] S.H. Strogatz, R.E. Mirollo, Splay states in globally coupled Josephson arrays: Analytical prediction of Floquet multipliers, Phys. Rev. E 47 (1) (1993) 220–227.
[19] S. Watanabe, S.H. Strogatz, Integrability of a globally coupled oscillator array, Phys. Rev. Lett. 70 (16) (1993) 2391–2394.
[20] S. Watanabe, S.H. Strogatz, Constants of motion for superconducting Josephson arrays, Physica D 74 (1994) 197–253.
[21] M. Wrage, P. Glas, D. Fischer, M. Leitner, D.V. Vysotsky, A.P. Napartovich, Phase locking in a multicore fiber laser by means of a Talbot resonator, Opt. Lett. 25 (19) (2000) 1436–1438.
[22] R.K. Dodd, J.C. Eilbeck, J.D. Gibbon, H.C. Morris, Solitons and Nonlinear Wave Equations, Academic Press, London, 1982.
[23] A.C. Newell, Solitons in Mathematics and Physics, SIAM, 1985.
[24] S. Flach, C.R. Willis, Discrete breathers, Phys. Rep. 295 (5) (1998) 181–264.
[25] P. Rosenau, J.M. Hyman, Compactons: Solitons with finite wavelength, Phys. Rev. Lett. 70 (5) (1993) 564–567.
[26] P. Rosenau, Nonlinear dispersion and compact structures, Phys. Rev. Lett. 73 (1994) 1737–1741.
[27] F. Cooper, H. Shepard, P. Sodano, Solitary waves in a class of generalized Korteweg–de Vries equations, Phys. Rev. E 48 (1993) 4027–4032.
[28] Y.S. Kivshar, Intrinsic localized modes as solitons with a compact support, Phys. Rev. E 48 (1993) R43–R45.
[29] B. Dey, A. Khare, Stability of compacton solutions, Phys. Rev. E 58 (1998) R2741–R2744.
[30] P.T. Dinda, T.C. Kofane, M. Remoissenet, Motion of compactonlike kinks, Phys. Rev. E 60 (1999) 7525–7532.
[31] P.T. Dinda, M. Remoissenet, Breather compactons in nonlinear Klein–Gordon systems, Phys. Rev. E 60 (1999) 6218–6221.
[32] M. Eleftheriou, B. Dey, G.P. Tsironis, Compactlike breathers: Bridging the continuous with the anticontinuous limit, Phys. Rev. E 62 (2000) 7540–7543.
[33] F. Cooper, J.M. Hyman, A. Khare, Compacton solutions in a class of generalized fifth-order Korteweg-de Vries equations, Phys. Rev. E 64 (2001) 026608.
[34] M. Manciu, S. Sen, A.J. Hurd, Crossing of identical solitary waves in a chain of elastic beads, Phys. Rev. E 63 (2001) 016614.
[35] J.C. Comte, Exact discrete breather compactons in nonlinear Klein–Gordon lattices, Phys. Rev. E 65 (2002) 067601.
[36] S. Takeno, Compacton-like modes in model dna systems and their bearing on biological functioning, Phys. Lett. A 339 (2005) 352–360.
[37] V.F. Nesterenko, Propagation of nonlinear compression pulses in granular media, J. Appl. Mech. Tech. Phys. 5 (1983) 733–743.
[38] A.N. Lazaridi, V.F. Nesterenko, J. Appl. Mech. Tech. Phys. 26 (1985) 405.
[39] C. Coste, E. Falcon, S. Fauve, Solitary waves in a chain of beads under Hertz contact, Phys. Rev. E 56 (5) (1997) 6104–6117.
[40] A. Rosas, K. Lindenberg, Pulse dynamics in a chain of granules with friction, Phys. Rev. E 68 (2003) 041304.
[41] S. Job, F. Melo, A. Sokolow, S. Sen, How Hertzian solitary waves interact with boundaries in 1D granular medium, Phys. Rev. Lett. 94 (2005) 178002.
[42] J. Rubinstein, Evolution equations for stratified dilute suspensions, Phys. Fluids A 2 (1) (1990) 3–6.
[43] P. Rosenau, A. Pikovsky, Phase compactons in chains of dispersively coupled oscillators, Phys. Rev. Lett. 94 (2005) 174102.
[44] K. Wiesenfeld, J.W. Swift, Averaged equations for Josephson junction series arrays, Phys. Rev. E 51 (2) (1995) 1020–1025.
[45] M. Abramowitz, I.A. Stegun, Handbook of Mathematical Functions, Department of Commerce USA, Washington, D.C., 1964.
[46] V.I. Petviashvili, Sov. J. Plasma Phys. 2 (1976) 257.
[47] V.I. Petviashvili, Multidimensional and dissipative solitons, Physica D 3 (1–2) (1981) 329–334.
[48] A. Chatterjee, Asymptotic solution for solitary waves in a chain of elastic spheres, Phys. Rev. E 59 (5) (1999) 5912–5919.
[49] T. Bohr, M.H. Jensen, G. Paladin, A. Vulpiani, Dynamical Systems Approach to Turbulence, Cambridge University Press, Cambridge, 1998.
[50] I. Aranson, L. Kramer, The world of the complex Ginzburg–Landau equation, Rev. Modern Phys. 74 (2002) 99–143.